Halsig *et al. Earth, Planets and Space* (2016) 68:106
DOI 10.1186/s40623-016-0482-5

Earth, Planets and Space

FULL PAPER Open Access

Using an atmospheric turbulence model for the stochastic model of geodetic VLBI data analysis

Sebastian Halsig*, Thomas Artz, Andreas Iddink and Axel Nothnagel

Abstract

Space-geodetic techniques at radio wavelength, such as global navigation satellite systems and very long baseline interferometry (VLBI), suffer from refractivity of the Earth's atmosphere. These highly dynamic processes, particularly refractivity variations in the neutral atmosphere, contribute considerably to the error budget of these space-geodetic techniques. Here, microscale fluctuations in refractivity lead to elevation-dependent uncertainties and induce physical correlations between the observations. However, up to now such correlations are not considered routinely in the stochastic model of space-geodetic observations, which leads to very optimistic standard deviations of the derived target parameters, such as Earth orientation parameters and station positions. In this study, the standard stochastic model of VLBI observations, which only includes, almost exclusively, the uncertainties from the VLBI correlation process, is now augmented by a variance–covariance matrix derived from an atmospheric turbulence model. Thus, atmospheric refractivity fluctuations in space and time can be quantified. One of the main objectives is to realize a suitable stochastic model of VLBI observations in an operational way. In order to validate the new approach, the turbulence model is applied to several VLBI observation campaigns consisting of different network geometries leading the path for the next-generation VLBI campaigns. It is shown that the stochastic model of VLBI observations can be improved by using high-frequency atmospheric variations and, thus, refining the stochastic model leads to far more realistic standard deviations of the target parameters. The baseline length repeatabilities as a general measure of accuracy of baseline length determinations improve for the turbulence-based solution. Further, this method is well suited for routine VLBI data analysis with limited computational costs.

Keywords: VLBI, Stochastic model, High-frequency atmospheric variations, Turbulence modeling

Introduction

The importance of space-geodetic techniques, such as global navigation satellite systems (GNSS) or very long baseline interferometry (VLBI), for the understanding of the Earth's atmosphere is steadily increasing. In particular, near real-time global positioning system (GPS) data can be used for numerical weather prediction applications (e.g., Crewell et al. 2008; Deng et al. 2011; Dousa and Bennitt 2013). However, at the same time dynamic processes in the neutral atmosphere critically affect the error budget of these space-geodetic techniques. For this reason, it is urgently necessary to use an adequate model for atmospheric conditions, in both the deterministic and stochastic components of the data analysis. Further, it is of great importance to provide an approach for operational and not just for experimental purposes.

The VLBI observable, the so-called delay, is given as the difference in arrival time of the observed signal from an extragalactic radio source at two different radio telescopes. The radio signal passes through the different atmospheric layers and, therefore, is affected by meteorological conditions. First, the ionosphere (between 80 and 1000 km above the Earth's atmosphere) is a dispersive medium, i.e., the phase velocity of a signal depends on its frequency. Thus, the delay due to the ionosphere can be corrected for using two frequencies in X-band

*Correspondence: halsig@igg.uni-bonn.de
Institute of Geodesy and Geoinformation, University of Bonn, Nussallee 17, 53115 Bonn, Germany

($f_X = 8.4$ GHz) and S-band ($f_S = 2.3$ GHz), respectively. In contrast to the ionosphere, the situation looks different in the neutral part of the atmosphere, particularly in the so-called troposphere, which is referred to the lower 10–15 km of the Earth's atmosphere. On the way through the troposphere, the radio signal is affected by the integral over all refractive indices along the signal path. Since the index of refraction is not equal to the refraction index in vacuum, the signal is subject to an additional delay as well as to bending and attenuation effects relative to a theoretical path in vacuum.

In the routine VLBI data analysis of the International VLBI Service for Geodesy and Astrometry (IVS, Schuh and Behrend 2012), the total tropospheric excess path length $\Delta L_t(\epsilon)$ for an observation of an arbitrary elevation ϵ is divided into a hydrostatic (index h) and a wet (index w) part, expressed as

$$\Delta L_t(\epsilon) = mf_h(\epsilon)\Delta L_h^z + mf_w(\epsilon)\Delta L_w^z. \quad (1)$$

Both components consist of a zenith delay correction (ΔL_h^z and ΔL_w^z, respectively) and a corresponding mapping function ($mf_h(\epsilon)$ and $mf_w(\epsilon)$, respectively), relating the zenith delay to an arbitrary elevation angle ϵ (Davis et al. 1985). On the one hand, the hydrostatic tropospheric delay in zenith direction (ZHD) mainly depends on the air pressure. The behavior of such meteorological data can be well identified using in situ measurements at the telescope site, and thus, the ZHD can be considered using an adequate model (e.g., the modified Saastamoinen model, see Davis et al. 1985). The wet part of the troposphere mainly depends on the water vapor content, which is unpredictable and highly variable in space and time (Elgered 1982). Thus, the zenith wet delay (ZWD) is routinely estimated as an additional parameter within a least-squares model or as a stochastic process in a filter estimation (e.g., Kalman filter, least-squares collocation, square-root information filter). In addition, troposphere gradients in north–south and east–west direction (G_{ns} and G_{ew}, respectively) can be estimated in the VLBI adjustment process to overcome azimuthal asymmetries [in Eq. (2), α denotes the azimuth] in the refractive index (MacMillan and Ma 1997). Thus, Eq. (1) is extended by an additional term yielding

$$\begin{aligned}\Delta L_t(\alpha,\epsilon) = {} & mf_h(\epsilon)\Delta L_h^z + mf_w(\epsilon)\Delta L_w^z \\ & + mf_g(\epsilon)[G_{ns}\cos(\alpha) + G_{ew}\sin(\alpha)].\end{aligned} \quad (2)$$

The order of magnitude of the hydrostatic component in zenith direction is about 2.3 m extra path length, and the additional zenith wet delay ranges from 0 cm in dry regions to 50 cm in the wet tropics. Thus, it is indispensable to account for this tropospheric delay in the VLBI data analysis. Actually, to go even further, atmospheric refraction is the limiting factor of any further improvements of the accuracy of telescope positions or Earth orientation parameters. However, today only long-periodic effects in the range of years to hours are considered routinely by the IVS. In contrast, small-scale refractivity fluctuations of minutes to sub-seconds due to turbulent swirls (or eddies) in the troposphere, in particular in the atmospheric boundary layer and in the free atmosphere, are largely ignored.

Further, dynamic processes in the neutral atmosphere induce spatial and temporal correlations between the observations. Concerning the stochastic model in the routine VLBI data analysis of the IVS, those correlations are also not taken into account. As a consequence, the standard deviations of the derived target parameters, such as telescope coordinates or Earth orientation parameters, are too optimistic.

To overcome this deficiency, in traditional VLBI data analysis the standard deviations derived from the VLBI cross-correlation process are inflated. This is achieved by adding either a constant term to the variances of the observations or doing a baseline-dependent re-weighting until the χ^2 value, defined as the quotient of the a posteriori and a priori variance factor, is approximately one.

On the theoretical side, more sophisticated strategies have been developed to improve the stochastic model of space-geodetic observations. For instance, Schön and Kutterer (2005) focus on the modeling of uncertainties due to remaining systematic errors of GPS data processing. In the case of VLBI, Tesmer (2004) and Tesmer and Kutterer (2004) propose a refinement of the routine stochastic model of VLBI observations by means of estimating variance and covariance components. Gipson et al. included station-dependent delay noise to the data analysis leading to more realistic standard deviations. For this purpose, they have distinguished two different types of delay noise: a constant additional component to deal with the clock behavior and an elevation-dependent noise term to consider atmospheric characteristics (Gipson 2006, 2007; Gipson et al. 2008).

To allow for a physically more reliable modeling of the stochastic properties in the VLBI data analysis, we now directly consider small-scale dynamic processes in the atmosphere. For this purpose, the stochastic model of VLBI observations is augmented by additional correlations due to high-frequency refractivity fluctuations which can be best described stochastically using the widely known Kolmogorov turbulence theory. Based on this turbulence theory, a few turbulence models have been developed over the last decades, which make either use of the so-called structure function or a power spectrum representation (cf. "Turbulence description" section). Treuhaft and Lanyi (1987) have pioneered

turbulence modeling for space-geodetic techniques leading to a turbulence-based variance–covariance matrix for tropospheric delays in VLBI. The model follows the Kolmogorov turbulence theory and describes the stochastic variations of the refractivity around its mean value. Romero-Wolf et al. (2012) presented a simplified modification of this model applied to observations of the VLBA (very-long baseline array) network. The Treuhaft and Lanyi (1987) model was also used by Pany et al. (2011) and Nilsson and Haas (2010) for extended simulation studies. In the latter one, particular consideration was also given to parametrization of specific station-dependent turbulence parameters, e.g., the structure constant C_n^2.

In addition, turbulence investigations have been carried out for GNSS observations. For instance, Schön and Brunner (2008) developed the so-called SIGMA-C model for GPS carrier phases, a variance–covariance model which also follows the turbulence theory of Kolmogorov and is based on the time-dependent integrated separation distance. In contrast to other applications, where the turbulent medium is generally assumed to be homogeneous and isotropic, inhomogeneity and anisotropy can be taken into account in this model. Halsig et al. (2014) used a SIGMA-C adapted model to investigate the stochastic model of VLBI observations. The main problem of turbulence modeling for most of these applications is obvious: Due to the necessary volume of integrations, which can only be solved numerically, they are mathematically difficult to handle and lead to large computational costs. By proposing an extension of the SIGMA-C model and using the so-called Matérn covariance family, Kermarrec and Schön (2014) developed a model which overcomes this issue.

In our endeavor to develop an operationally efficient method for turbulence modeling in routine mass analysis of VLBI observing sessions, we devise a VLBI-specific version of the Kermarrec and Schön (2014) model. With this, we generate a suitable variance–covariance matrix in the stochastic model of VLBI data analysis and, therefore, far more realistic standard deviations of the derived target parameters within the parameter estimation process. So, one of the key objectives of this paper is to develop a suitable strategy to consider atmosphere-based correlations between VLBI observations in an operational way, i.e., it must be guaranteed that the model is mathematically easy to handle and the use of a fully populated variance–covariance matrix is feasible without to much computational effort.

This contribution is organized as follows. In "Turbulence description" section, an introduction to the Kolmogorov turbulence theory and strategies for modeling atmospheric turbulence are presented. It is followed by "Data analysis setup" section on the description of the data analysis setup. In "Results" section, the results of the VLBI data analysis using a modified stochastic model with external physical correlations are illustrated for several VLBI observation campaigns consisting of different network geometries and for different solution setups. Finally, a conclusion and ideas for future work are given in "Conclusions" section.

Turbulence description

Electromagnetic waves originating from natural or artificial sources, such as extragalactic radio sources or satellites, pass through the atmosphere to an antenna on the Earth's surface. These waves are affected by atmospheric conditions leading to attenuation, scintillation and delay of the signal. In this context, the atmosphere is subdivided into its main components, the neutral atmosphere and the ionosphere. The effects of the ionosphere caused by the ionization by solar radiation are frequency dependent and can therefore be considered using two different frequencies. In contrast, the neutral atmosphere is a non-dispersive medium and the long-periodic variations as well as small-scale fluctuations caused by atmospheric turbulence cannot be calibrated by in situ measurements. For this reason, the long-periodic effects are considered in the routine VLBI and GNSS data analysis in a deterministic sense within the parameter estimation procedure. The short-periodic fluctuations on the other hand mainly depend on variations of the refractive index induced by turbulent motions. These are generally regarded as randomly varying in space and time and thus have to be described stochastically (Ishimaru 1991).

In order to receive a mathematical description of a random medium such as the refractivity index n, it is separated into two components $n = \bar{n} + \Delta n$ (as first proposed by Reynolds in 1895, cf. Tatarskii 1971). While $\bar{n}$ describes the mean value in steady state and defines a deterministic part, Δn is characterized by rapid fluctuations and defines a stochastic component. The phenomena described by Δn are referred to turbulence and can be represented as the interaction or superposition of turbulent swirls of different length scales, so-called eddies, i.e., an arbitrary flow pattern characterized by its size (Batchelor 1950). According to Wheelon (2004, p. 83), the shape and size of the eddies depend on the altitude. In the atmospheric boundary layer (0–2 km of altitude), the eddies are assumed to be small and not far from symmetrical, while the irregularities in the free atmosphere are highly anisotropic, i.e., the eddies become more flattened in horizontal direction (see Fig. 1).

For the sake of a better visualization of the eddy variations in the atmospheric boundary layer, turbulent processes are often referred to the energy cascade theory

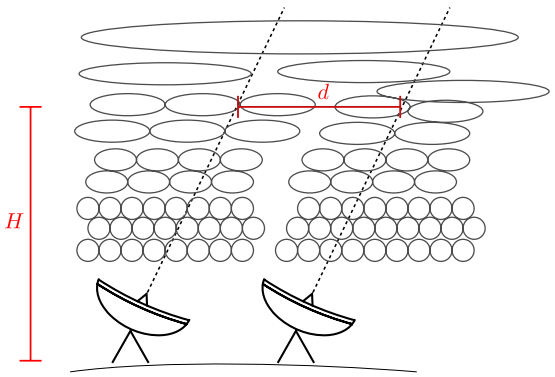

Fig. 1 Concept of eddies. Eddy size and flattening with height, according to Wheelon (2004, p. 83)

(Kolmogorov 1941), as depicted in Fig. 2. The model associates the amount of turbulent energy with different eddy scales. Starting at the outer scale wavenumber, or formulated differently, at the point, at which the eddy size is equal to the outer scale length L_0, a small fraction of the kinetic energy in the ambient wind field is converted into turbulent energy producing initial inhomogeneities (energy injection). Since these eddies are not stable, they immediately begin to break up and subsequently transfer their energy to turbulent elements of smaller and smaller scale (inertial subrange). The shape of the eddies becomes more and more symmetrical. The redistribution during the decay cascade continues until the eddy size is approximately equal to the inner length scale l_0, at which their remaining energy is dissipated into heat (energy dissipation).

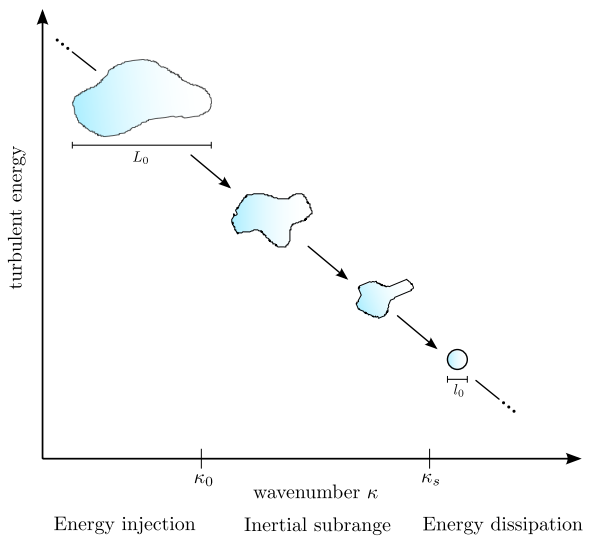

Fig. 2 Cascade model. The energy cascade model of Kolmogorov describes the process of turbulent decay. As soon as the turbulent eddies are created, they break up into smaller and more symmetric eddies until their energy is dissipated as heat (according to Wheelon 2004, p.29)

According to Wheelon (2004, p. 205f), the free atmosphere plays the dominant role for interferometry based on microwave signals, since it contains most of the ray path. The turbulent eddies are highly anisotropic, i.e., highly flattened in the horizontal plane, and exhibit significant correlations over hundreds of kilometers.

Modeling atmospheric turbulence

In the following, our attention is devoted to the spatial dependence of the observations derived by two antennas operating at two positions $\mathbf{r_1}$ and $\mathbf{r_2}$ and separated by $\mathbf{d}$ in a random medium, which similarly can be described by the spatial covariance function

$$\mathcal{C}_n(\mathbf{r_1}, \mathbf{r_2}) = \langle \Delta n(\mathbf{r_1}, t) \Delta n(\mathbf{r_2}, t) \rangle, \tag{3}$$

where $\langle \ldots \rangle$ denote the ensemble average (ensemble is defined as all possible configurations of the random medium). In general, the atmosphere is assumed to be homogeneous and isotropic. Homogeneity can be interpreted as the spatial analogy of the stationarity, i.e., the covariance function does not depend on the positions $\mathbf{r_1}$ and $\mathbf{r_2}$ but solely on the baseline separating these positions. Further, a medium is also defined as isotropic, if the vertical scale is the same as both horizontal scales, i.e., the covariance function only depends on the magnitude of the baseline, not on its orientation Wheelon (2004, p. 15ff). Then, including both assumptions, Eq. (3) becomes

$$\mathcal{C}_n(\mathbf{d}) = \langle \Delta n(\mathbf{r}, t) \Delta n(\mathbf{r} + \mathbf{d}, t) \rangle. \tag{4}$$

According to Tatarskii (1971), the atmosphere can be considered as a "locally homogeneous random medium with smoothly varying characteristics" leading to a separation of the random medium into a varying mean and a rapidly changing fluctuating component. Thus, the slowly varying term is canceled out by taking the difference and assuming a sufficient similarity for both positions $\mathbf{r_1}$ and $\mathbf{r_2}$. This leads to the structure function description:

$$\mathcal{D}_n(\mathbf{r_1}, \mathbf{r_2}) = \langle [\Delta n(\mathbf{r_1}, t) - \Delta n(\mathbf{r_2}, t)]^2 \rangle. \tag{5}$$

Further, the spatial covariance function in Eq. (3) can be expressed as a power spectral density by using a three-dimensional Fourier transform (see Wheelon 2004, p. 21), yielding

$$\langle \Delta n(\mathbf{r_1}, t) \Delta n(\mathbf{r_2}, t) \rangle = \int_0^\infty \int_0^\infty \int_0^\infty \kappa \Phi_n(\kappa) e^{i\kappa(\mathbf{r_1} - \mathbf{r_2})} \mathrm{d}^3\kappa. \tag{6}$$

Using the wavenumber spectrum representation, the random medium is completely described by the turbulence spectrum $\Phi_n(\kappa)$, where $\kappa = [\kappa_x, \kappa_y, \kappa_z]$ denotes the wavenumber vector. As shown by dimensional analysis in Kolmogorov (1941), the energy spectrum should follow a power law process. Thus, the von Karman spectrum is used as a power spectral density description (see Wheelon 2004, p. 41),

$$\Phi_n(\kappa) = \frac{0.033 C_n^2}{\left(\kappa_x^2 + \kappa_y^2 + \kappa_z^2 + \kappa_0^2\right)^{\frac{11}{6}}}, \tag{7}$$

which is valid for the inertial subrange and the energy input region, $0 < \kappa < \kappa_s$ (where κ_0 and κ_s denote the corresponding wavenumber to the outer and inner scale length L_0 and l_0, respectively).

In Eq. (7) again homogeneity and isotropy are assumed. Since Tatarskii (1971) defined the atmosphere as a "locally homogeneous random medium with smoothly varying characteristics," we can again subdivide $\Phi_n(\kappa, \frac{\mathbf{r_1}+\mathbf{r_2}}{2})$ into a slowly varying component $\overline{\Phi}_n(\kappa)$ and a rapidly fluctuating term $C_n^2(\frac{\mathbf{r_1}+\mathbf{r_2}}{2})$ (Kermarrec and Schön 2014),

$$\Phi_n\left(\kappa, \frac{\mathbf{r_1}+\mathbf{r_2}}{2}\right) = C_n^2\left(\frac{\mathbf{r_1}+\mathbf{r_2}}{2}\right)\overline{\Phi}_n(\kappa). \tag{8}$$

To deal with anisotropy, the so-called stretched wavenumber coordinates are introduced according to Wheelon (2004, p. 42ff). The stretching factors a, b and c describe the flattening of the eddies in both the horizontal and the vertical directions, leading to

$$\Phi_n(\kappa) = \frac{0.033 C_n^2 abc}{\left(a^2\kappa_x^2 + b^2\kappa_y^2 + c^2\kappa_z^2 + \kappa_0^2\right)^{\frac{11}{6}}}. \tag{9}$$

Up to now, we have considered refractive index fluctuations, particularly large horizontal flattened eddies in the free atmosphere, which distort the arriving plane wave front of VLBI observations. Integrating these refractivity fluctuations along the line of sight yields the signal phase variations. According to Wheelon (2004, p. 206), the phase covariance function can be expressed as

$$\mathcal{C}_\varphi = k^2 \int_0^\infty \mathrm{d}s_1 \int_0^\infty \mathrm{d}s_2 \int_{-\infty}^{\infty}\int_{-\infty}^{\infty}\int_{-\infty}^{\infty} \times\ \kappa\Phi_n\left(\kappa, \frac{\mathbf{r_1}+\mathbf{r_2}}{2}\right) e^{i\kappa(\mathbf{r_1}+\mathbf{r_2}-\mathbf{d})}\mathrm{d}^3\kappa. \tag{10}$$

Since the refractive index along the path is fluctuating, the signal phase is also affected by temporal variations. To describe the temporal variability, we use the time-shifted phase covariance expression

$$\mathcal{C}_\varphi(\tau) = \langle\varphi(t)\varphi(t+\tau)\rangle, \tag{11}$$

which primarily depends on the wind fields in the atmosphere. Thus, the widely known frozen flow hypothesis of Taylor (1938) is used to describe temporal variations in a random medium. It postulates that the entirety of turbulent air mass is frozen during the observing period and transported horizontally at a constant wind velocity without any deformation. Consequently, the motion of the entire turbulence mass is equivalent to a parallel shifting of the ray path, i.e., the phase covariance at time t and $t+\tau$, respectively, has to be identical to the spatial correlation between these rays with separation distance $\mathbf{d} = \mathbf{v}\tau$ (see Fig. 3). Thus, the spatial covariance function can be extended by this additional displacement, yielding

$$\langle\Delta n(\mathbf{r}, t)\Delta n(\mathbf{r}+\mathbf{R}, t+\tau)\rangle = \int_{-\infty}^{\infty}\int_{-\infty}^{\infty}\int_{-\infty}^{\infty} \kappa\Phi_n(\kappa, \mathbf{r}) e^{i\kappa(\mathbf{R}+\tau\mathbf{v})}\mathrm{d}^3\kappa. \tag{12}$$

An alternative description for the covariance function of the phase difference is derived by using the power spectrum $\mathcal{W}_\varphi(\omega)$, which is intimately connected by the Wiener–Khintchine theorem (Wheelon 2004, p. 257):

$$\mathcal{W}_\varphi(\omega) = \int_{-\infty}^{\infty} d\tau e^{i\omega\tau}\langle\varphi(t)\varphi(t+\tau)\rangle\,\mathrm{d}\tau. \tag{13}$$

According to Wheelon (2004, Sec. 6.5) and Kermarrec and Schön (2014), the spectrum of phase measurements can be expressed as

$$\mathcal{W}_\varphi(\omega) = \frac{2.192 H k^2 C_n^2 c a^{-\frac{5}{3}} \nu^{\frac{5}{3}}}{\sin^2(\epsilon)\left[\omega^2 + \left(\frac{\kappa_0\nu}{a}\right)^2\right]^{\frac{4}{3}}}, \tag{14}$$

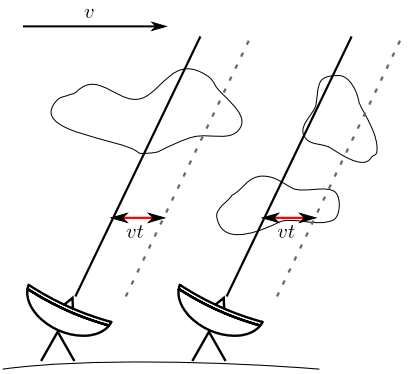

Fig. 3 Taylor's frozen flow model. Taylor's frozen flow hypothesis assumes the entirety of turbulent medium to be frozen and traveling in the direction, in which the wind blows with a constant velocity (according to Wheelon 2004, p. 244)

which is valid for a slab model, i.e., assuming the von Karman spectrum, the wind velocity v to be non-varying and C_n^2 to be constant up to the tropospheric height H and vanishing above. Anisotropy and homogeneity are taken into account. Kermarrec and Schön (2014) found that the corresponding covariance,

$$\mathbf{C}(t,t+\tau) = 0.7772\frac{k^2HC_n^2c}{\sin(\epsilon_i(t))\sin\left(\epsilon_j(t+\tau)\right)} \times \kappa_0^{-\frac{5}{3}}\left(\frac{\kappa_0 v\tau}{a}\right)^{\frac{5}{6}}K_{\frac{5}{6}}\left(\frac{\kappa_0 v\tau}{a}\right), \quad (15)$$

is a so-called Matérn covariance function (Matérn 1960) with a smoothness parameter $\nu = \frac{5}{6}$ and a Matérn correlation time $\mathcal{T} = \frac{1}{\alpha}$, where $\alpha = \frac{\kappa_0 v}{a}$ and $\kappa_0 = \frac{2\pi}{L_0}$. Here, $K_{\frac{5}{6}}$ represents the modified Bessel function of second kind (Abramowitz and Segun 1964). The corresponding variance expression reads

$$\mathbf{C}(t,t) = 0.782\frac{k^2HC_n^2c\kappa_0^{-\frac{3}{5}}}{\sin^2(\epsilon_i(t))}. \quad (16)$$

Equations (16) and (15) are used to generate a variance–covariance matrix based on high-frequency refractivity fluctuations in the neutral atmosphere, which is then, in a next step, incorporated in the VLBI estimation procedure. The turbulence-based variance–covariance matrix is therefore added to the routine variance–covariance matrix of the Gauß Markov model, which is currently a pure diagonal matrix and includes, almost exclusively, the uncertainties from the VLBI correlation process.

Turbulence parametrization

The most crucial point in the turbulence-based model is the determination of the turbulence parameters, particularly the "scaling parameters" C_n^2, H and a, b, c as well as the wind parametrization. Although the structure constant decreases with height from $C_n^2 = 10^{-18}\,\mathrm{m}^{-\frac{2}{3}}$ at 10 km height to $C_n^2 = 10^{-14}\,\mathrm{m}^{-\frac{2}{3}}$ at 1 km height, C_n^2 can be assumed to be constant up to the tropospheric height $H \approx$ 1000–2000 m and zero above (e.g., Schön and Brunner 2008). In principle, there are different methods to estimate the structure constant at the specific VLBI site, e.g., from water vapor radiometer, radiosonde or GPS data (Nilsson and Haas 2010). However, for a suitable description of the turbulent behavior over a VLBI station, such sensors have to be available near to these radio telescopes, which is usually only the case for GPS sensors, if at all. However, particularly with regard to the VLBI Global Observing System (VGOS, e.g., Niell et al. 2013), the next-generation VLBI system, which leads to a significant increase of observations and a better coverage, the estimation of C_n^2 parameters may be possible using VLBI observations. Here, especially short baselines of so-called twin telescopes in local networks should be used to determine turbulence effects assuming that other atmospheric effects could be neglected in such local applications. The parameters a, b and c describing the flattening of the turbulent media are chosen to $a = b > c$ due to the increasing horizontal flattening with height up to $a = b = 100\,c$ (Wheelon 2004).

The wind is parametrized as a constant horizontal wind velocity and a wind direction, which is defined by the separation distance $d_H(t)$ between the two radio signals at height H. Assuming the so-called free atmosphere from 1000 to 3000 m to be crucial inducing physical correlations between the observations and determining $v \approx 8\,\frac{m}{s}$, which corresponds approximately to the geophysical wind at that height, these parametrization may be sufficient.

However, when additionally considering the atmospheric boundary layer below 1000 m, which is easy possible with this model, or when considering more global network geometries, which is the standard case in VLBI, the parametrization described above should be specified, because the meteorological conditions may not be the same at two VLBI stations of a baseline. This issue will be investigated further in the near future, but is not part of this study.

Data analysis setup

In the following, our VLBI data analysis setup will be briefly described. Here, the VLBI target parameters such as telescope positions or Earth orientation parameters (EOP) are estimated in a least-squares method using a Gauss Markov model (Koch 2013). In addition to the target parameters, necessary clock and atmospheric model parameter corrections are estimated as well. In the case, which is currently standard, the weight matrix of the Gauss Markov model is a pure diagonal matrix.

The analysis of the observed group delays is performed following the conventions of the International Earth Rotation and Reference Systems Service (IERS, Petit and Luzum 2010). The parametrization setup for single-session VLBI data analysis has been chosen with respect to the routine data analysis strategies of the IVS. First, the coordinates of the radio telescopes and EOPs are estimated with respect to the current version of the International Terrestrial Reference Frame (ITRF, Altamimi et al. 2011). In order to eliminate the datum defect, i.e., to remove the natural VLBI rank deficiency, additional no-net-rotation (NNR) and no-net-translation (NNT) conditions (Angermann et al. 2004) have been applied. Polar motion and UT1-TAI are parametrized with offsets and

rates, while radio source coordinates are not estimated, but fixed to the International Celestial Reference Frame (ICRF2, Fey et al. 2015).

In addition to the target parameters, we need to estimate further auxiliary quantities such as clock and atmospheric model correction parameters. The clock parameters are modeled by a second-order polynomial and additional continuous piecewise linear functions (CPWLF), i.e., linear splines (De Boor 1978), with a temporal resolution of 60 min. Finally, the wet component of the atmospheric delay is estimated in zenith direction and parametrized as an offset as well as CPWLFs with a resolution of 60 min. For the mapping of the tropospheric wet delay from zenith to the slant direction (i.e., the line of sight), the Vienna Mapping Function 1 (VMF1, Böhm et al. 2004) is used, which is derived from a numerical weather model of the European Centre for Medium-Range Weather Forecast (ECMWF). Further, azimuthal gradients are estimated as daily CPWLFs. In order to stabilize the equation system, the clock, ZWD and gradient parameters are supplemented by additional constraints which affect the equation system as weighted pseudo-observations.

The model parameters describing the state of the turbulent atmosphere have been kept very simple and have been chosen to be the same for all stations. A constant structure constant $C_n^2 \approx 1e^{-14}\,\mathrm{m}^{-\frac{2}{3}}$ is used, the effective tropospheric height is set to $H = 2000\,\mathrm{m}$, and a constant wind velocity $v = 8\,\frac{m}{s}$ in horizontal direction is assumed. The stretching factors describing the flattening of the turbulent eddies have been chosen to $a, b = 1$ and $c = 0.01$ to consider for anisotropy in the free atmosphere. Of course, these values are based on a model parametrization, which is only an approximation to the truth. However, they are suited to demonstrate the general functionality of the turbulence-based approach based on experience-related values. Again, the influence of the parametrization will be investigated further in the future, but is not part of this study.

Results

The standard VLBI stochastic model includes, almost exclusively, the uncertainties from the VLBI correlation process. In our case, this model is augmented by a variance–covariance matrix derived from the model according to Eqs. (15) and (16) to manage high-frequency refractivity fluctuations in the atmosphere. Through this approach, the standard deviations of the estimated parameters become more realistic, as depicted exemplarily in Fig. 4 for the 15-day continuous VLBI campaign in October 2002 (CONT02). Here, the standard deviations of the vertical component of the station coordinates are illustrated as differences between several solutions refining the stochastic model and the solution based on the routine data analysis of the IVS (see Table 1 or the description further down in the text). According to Böckmann et al. (2010), the average noise level of about 115 IVS sessions in terms of WRMS of single-session position estimates, computed after removing offset, rate and annual signal is about 4.5 mm for the horizontal and

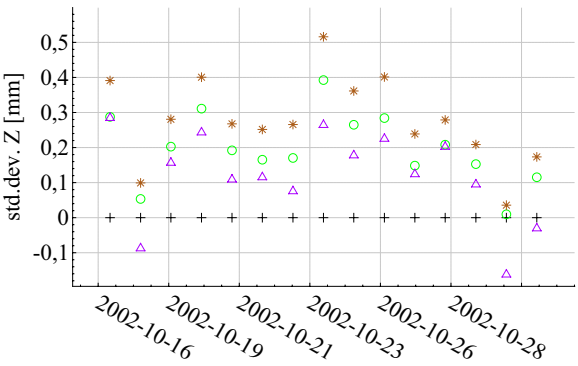

Fig. 4 Level of uncertainty for telescope coordinates. Differences in standard deviations of the vertical component of the station coordinates between a simple solution with a constant additional noise term (*purple triangles*), the Gipson et al. (2008) approach (*green circles*) and the turbulence-based solution (*brown stars*) with respect to the reference solution (*black crosses*)

Table 1 Different solution setups including the reference solution and different strategies to refine the stochastic model of VLBI observations

	Solution type	χ^2 (–)	WRMS (ps)
A	Reference solution	2.32	34.53
B	Constant additional noise: 1 cm	0.86	42.46
C	Gipson et al. (2006–2008) constant and elevation-dependent noise	1.13	36.24
D	Turbulence-based correlations	1.18	34.93

The mean χ^2 and WRMS values over about 2700 VLBI sessions between 1993 and 2014 are illustrated for all solution setups

about 6.5 mm for the vertical component. Using a modified stochastic model, i.e., either the turbulence-based model or the Gipson et al. (2008) model, the level of uncertainty is getting closer to these values with very few exceptions, assuming that the noise level becomes more realistic.

To validate the turbulence model, we made use of about 2700 VLBI sessions between 1993 and 2014, provided by the IVS (Nothnagel et al. 2015). These include several observation campaigns consisting of different network geometries. In addition to the routine 24 h IVS VLBI sessions, specially designed observation campaigns are set up at the Geodetic Observatory Wettzell (Bavarian Forest, Germany). These so-called WHISP sessions (Wettzell high-speed VLBI session) consist of only one short 123-m-long baseline between the 20-m radio telescope Wettzell (RTW) and the north antenna of the twin telescope Wettzell (TTW-1, Schüler et al. 2015). The advantage of these WHISP sessions is the large number of observations per telescope compared with other VLBI sessions. Further, these sessions allow for a validation of the turbulence model in a local application.

For all VLBI data, we computed several solutions with different setups (see Table 1). Since the traditional stochastic model of VLBI observations only consists of uncertainties due to the VLBI correlation process and an additional noise term (see "Introduction" section), we made use of different noise term strategies to validate our turbulence-based approach. First, we generate a simple approach without using any kind of additional noise term, referred to as reference solution (A) in the following. The most simple approach (B) of re-weighting the observations is to add the same constant noise term for all observations and sessions, which is chosen to ≈1 cm. However, this strategy is applied here not only for validation purposes; it is common practice in some widely spread VLBI software packages.

A further solution has been processed following the model of Gipson et al. (2008), who added station-dependent noise, which then leads to an increase in the standard deviations. Here, a constant and an elevation-dependent noise terms are added to the standard deviations, which correspond to the clock and troposphere model parameter, respectively. The order of magnitude of both noise terms is related to the analyses in Gipson (2006), Gipson (2007) and Gipson et al. (2008). Finally, we formed a solution incorporating our fully populated turbulence-induced variance–covariance matrix (D) in the stochastic model of VLBI observations. In contrast to the other solution setups, here the observations are not weighted by any additional noise terms. Concerning the turbulence description, we used the same model parametrization for all stations (see "Turbulence parametrization" section)

In order to assess the quality of the different strategies for refining the stochastic model, three statistical criteria are used: (a) the χ^2 value, (b) the weighted root mean squared (WRMS) of the post-fit residuals and (c) the baseline length repeatabilities. First, the χ^2 value is defined as the quotient of the a posteriori $\tilde{\sigma}^2$ and the a priori variance factor σ_0^2,

$$\chi^2 = \frac{\tilde{\sigma}^2}{\sigma_0^2}, \tag{17}$$

and gives an information whether the global test for an adjustment is fulfilled or not. Assuming $\chi^2 \approx 1$ (referred to as target value and represented as a gray dashed line in Figs. 5a, 7a, respectively) indicates that the global test is fulfilled, i.e., the deterministic and stochastic model assumptions are valid. The a posteriori variance factor in Eq. (17) can be written as

$$\tilde{\sigma}^2 = \frac{\left\langle \mathbf{A}^T\mathbf{x} - \mathbf{b} \right\rangle_{\mathbf{\Sigma}_{ll}^{-1}}}{f}, \tag{18}$$

where $\mathbf{A}$ describes the Jacobian matrix, $\mathbf{b}$ is the observed-minus-computed vector with the corresponding variance–covariance matrix of observations $\mathbf{\Sigma}_{ll}$, the vector of parameters is denoted as $\mathbf{x}$ and f gives the degrees of freedom.

Second, the WRMS scatter per solution based on the post-fit residuals r_i can be written as

$$WRMS = \sqrt{\frac{\sum_i r_i^2 \frac{1}{\sigma_i^2}}{\sum_i \frac{1}{\sigma_i^2}}}, \tag{19}$$

where the vector of residuals is defined by

$$\mathbf{r} = \mathbf{A}^T\mathbf{x} - \mathbf{b}. \tag{20}$$

The χ^2 values and WRMS post-fit residuals are shown in Fig. 5a, b, respectively. The reference solution is illustrated as black crosses, purple triangles denote the setup adding 1-cm constant noise terms for all observations. The approach following Gipson et al. (2008) is marked as green circles. Finally, the turbulence-based solution is represented by brown stars. In addition, Table 1 shows the WRMS post-fit residuals of the delay observables as well as the χ^2 values as mean values per solution setup over the 2700 VLBI sessions.

Compared with the reference solution (black, $\chi^2 \approx$ 2–5), the χ^2 values are generally reduced as soon as an arbitrary refinement strategy is used. However, considering the mean values in Table 1, it becomes obvious that in case of the easiest approach (purple) $\chi^2 < 1$ indicating an overestimation in the data analysis. In this context,

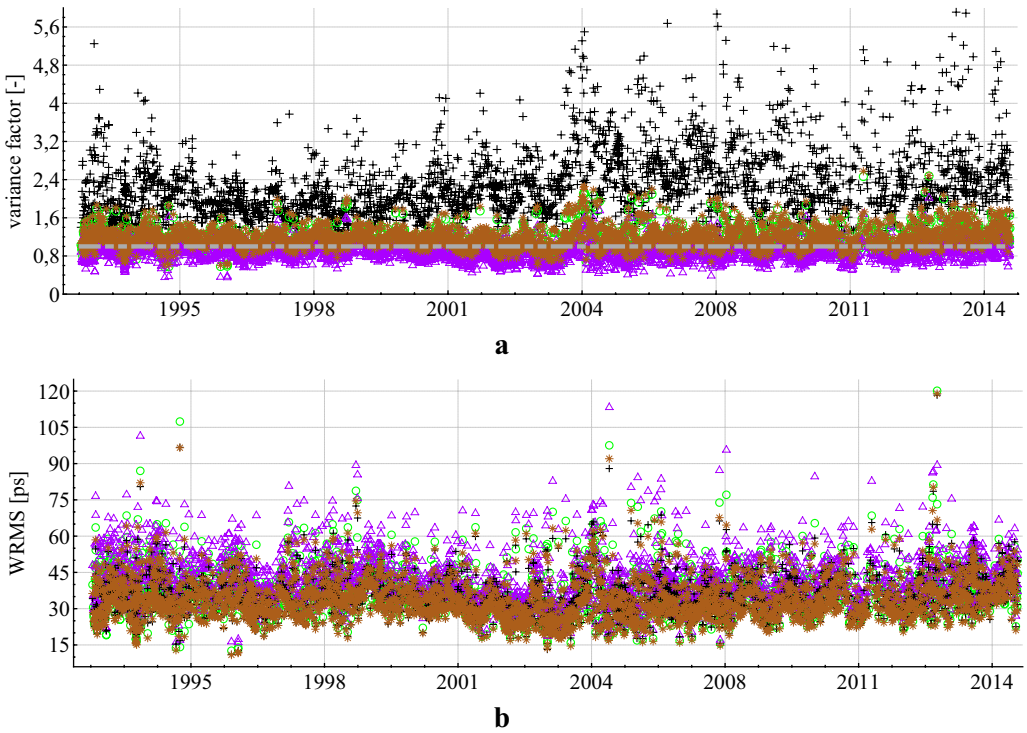

Fig. 5 χ^2 values and WRMS post-fit residuals. **a** χ^2 values and **b** WRMS post-fit residuals for about 2700 VLBI sessions between 1993 and 2014 and different solution setups including a reference solution (*black crosses*), a simple solution with a constant additional noise term (*purple triangles*), the Gipson et al. (2008) approach (*green circles*) and the turbulence-based solution (*brown stars*). The *gray dashed line* in **a** represents $\chi^2 = 1$

overestimation means that the a priori model is too idealistic in the sense of too enthusiastic initial weights, which is compensated for in the estimation procedure. Conversely, underestimation would imply a too pessimistic a priori modeling and too unpromising initial weights. Although only a very simple model is used in this case, the χ^2 values are quite close to one. Similarly positive results can be obtained by the turbulence-based solution (brown) and the Gipson et al. (2008) approach (green), where the χ^2 values are approximately one indicating a realistic adjustment, but they are still slightly to high. However, in case of the turbulence model, this is not surprising when recalling the fact that only atmospheric effects are considered in the stochastic model, which are the dominant but not sole error source in VLBI data analysis. For instance, the uncertainties of clock behavior are neglected in the stochastic model. Additionally, the parameters describing the atmospheric turbulence, C_n^2, H, a, b, c and ν are quite simple up to now.

Considering the WRMS post-fit residuals, it is obvious that, compared with the other refinement strategies, the use of a turbulent variance–covariance matrix produces the lowest WRMS post-fit residuals. Expressed in numbers and, for instance, compared with the Gipson et al. (2008) approach, the turbulence-based solution improves by 9.5 ps in quadrature. Nevertheless, both solutions are significantly better than the solution adding constant noise terms only, where the mean WRMS value is degraded by about 24 and 22 ps in quadrature with respect to the turbulent-based and Gipson et al. (2008) approach, respectively. Surprisingly perhaps, the WRMS post-fit residuals for the reference solution are on the same level as for the turbulence-based solution. However, keeping in mind that the χ^2 values are too high by the factor of two or even more, it should be discouraged to use the different validation criteria separately.

It is common practice in the VLBI community to measure the accuracy of baseline length determinations in terms of their repeatabilities. Thus, we finally use the baseline length repeatabilities, which can be regarded as the standard deviation for an individual baseline after removing a linear trend from a time series of baseline lengths. Figure 6a shows the baseline length repeatabilities for all baselines, which occur in at least 30 sessions, for the same 2700 VLBI sessions and solution setups as used before. An exponential trend is fitted to the data, which is included as solid lines in Fig. 6a. Again, the turbulence-based solution and the Gipson et al. (2008) approach lead to the best results. For a better visualization, the baseline length repeatabilities shown in Fig. 6a

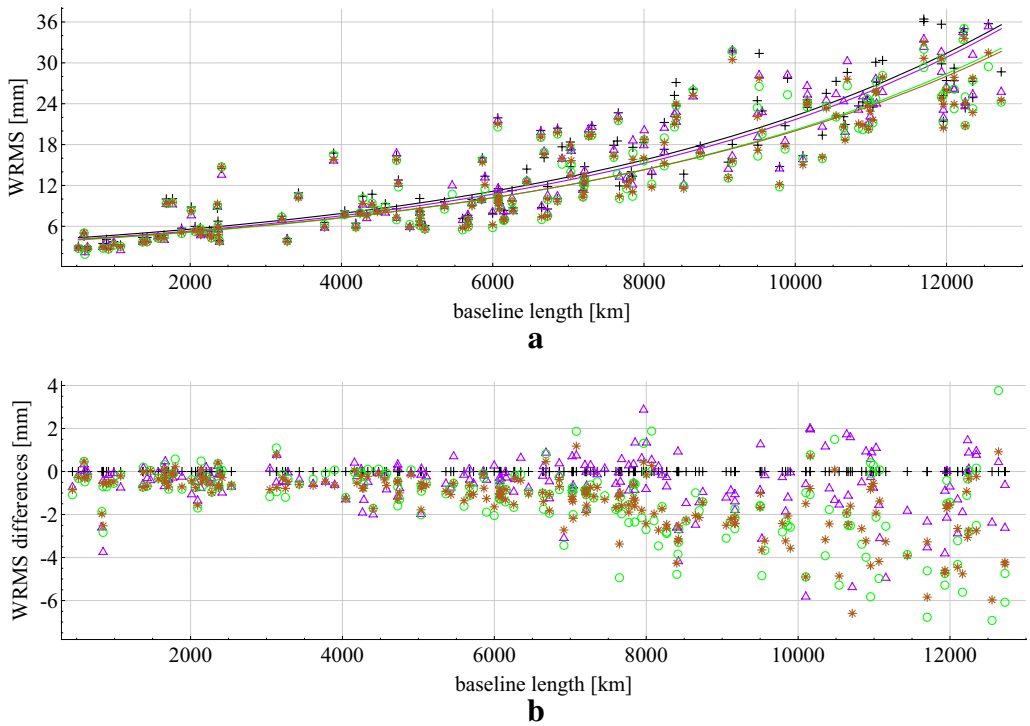

Fig. 6 *Baseline* length repeatabilities. **a** *Baseline* length repeatabilities for about 2700 VLBI sessions between 1993 and 2014 and different solution setups including a reference solution (*black crosses*), a simple solution with a constant additional noise term (*purple triangles*), the Gipson et al. (2008) approach (*green circles*) and the turbulence-based solution (*brown stars*). For each solution, an exponential trend is fitted to the data (*solid lines*). **b** Baseline length repeatabilities of **a** as differences with respect to the reference solution

are calculated as differences with respect to the reference solution. The result is illustrated in Fig. 6b, where negative WRMS differences indicate and improvement, whereas positive values show a degradation in baseline length repeatabilities. It becomes obvious that including only a constant noise term to the variances of the observations, the results are getting better or worse to the same extent. Contrary, using the turbulence-based model as well as the Gipson et al. (2008) model leads to a clear improvement in (almost) all cases. Expressed in numbers, and compared with the reference solution, the baseline length repeatabilities improve for 50.3 % of all baselines by at least 1 mm when using a turbulence-based stochastic model, whereas no baselines lead to a degradation by at least 1 mm. 49.7 % of the baseline remain unchanged. This result is quite similar if we compare the turbulence-based solution to the solution at constant noise level (improvement of 35.6 % of the baselines versus degradation of 3.4 % of the baselines by at least 1 mm; 61 % of the baselines remain unchanged), which, as already stated, is not unusual in practice.

In addition to the traditional VLBI networks, we analyzed two short baselines in Hobart, Tasmania, and Wettzell, Germany. Since the turbulence model of Kermarrec and Schön (2014) was originally developed for small-scale networks, these sessions are an opportunity to validate the VLBI-adapted turbulence model for local VLBI networks as well.

First, we made use of two specially designed so-called WHISP sessions observed on August 27, 2014, and October 23, 2014, respectively, which only consists of one short baseline between the 20-m radio telescope and the north antenna of the twin telescope at the Geodetic Observatory in Wettzell. Table 2 lists the χ^2 values and WRMS post-fit residuals for these sessions. The results look different to the global analysis. The χ^2 values derived from the reference solution are approximately 1.3 and 1.8. Introducing a constant term to the variances of the observations or following the Gipson et al. (2008) model, the χ^2 values are clearly too small, particularly in case of the WHISP001 session ($\chi^2 < 0.5$), leading to an overestimation in these solutions. Using the turbulence model, the χ^2 values are again approximately one. Regarding the WRMS post-fit residuals, the situation appears similar to the global case, at least for WHISP002. In contrast, the WRMS post-fit residuals for WHISP001 are sharply improved using the turbulence-based solution in comparison with all other approaches including the reference solution.

Table 2 Different solution setups including the reference solution and different strategies to refine the stochastic model of VLBI observations

	Solution type	χ^2 (–)		WRMS (ps)	
		WHISP001	WHISP002	WHISP001	WHISP002
A	Reference solution	1.27	1.76	14.23	22.26
B	Constant additional noise: 1 cm	0.32	0.48	15.01	23.29
C	Gipson et al. (2006–2008) constant and elevation-dependent noise	0.47	0.79	13.61	23.51
D	Turbulence-based correlations	0.96	1.02	11.55	22.53

The χ^2 and WRMS value for two specially designed WHISP sessions on August 27 and October 23, 2015, are illustrated for all solution setups

We could confirm these results by using a second short baseline between the two VLBI stations HOBART26 and HOBART12 observed during the continuous VLBI campaign in May 2014 (CONT14). The χ^2 values for the same set of solutions are shown in Fig. 7a. Please note that in this case the Gipson et al. (2008) approach acts different since the solution leads, in contrast to the WHISP baseline, to an underestimation. The WRMS post-fit residuals in Fig. 7b confirm the previous findings.

It is worth mentioning that, of course, we could vary the amount of re-weighting the variances of observations in the other models until the $\chi^2 \approx 1$. However, it should in fact be pointed out that there is no valid general approach and solely the turbulence-based solution is able to handle this situation in global and local networks.

Usually, the use of a fully populated variance–covariance matrix in the stochastic model represents the restrictive factor keeping the computational costs to a limited extent. In this regard, we made use of several VLBI sessions with different quantities of data to validate our approach. In a small network consisting of three stations and about 400 observations, there is almost no loss in time. Regarding for instance the WHISP sessions with over 1000 observations on one baseline, there is hardly no difference between the solutions with and without turbulent correlations. Increasing the number of observation (i.e., 5000 and more), the loss of time is increasing up to the factor 5. In this case, the turbulence-based solution also requires a little more time than the other strategies taken for validation purposes (i.e., the Gipson et al. (2008) model and the approach with constant additional noise), which is of course due to the correlations only taken into account by the turbulence-based model. However, the maximum computational effort is still not higher than 60 s in these cases. Thus, the turbulence model is feasible for common VLBI sessions without too much computational effort. However, in case of the new VGOS networks and the significantly increasing number of observations, further optimization strategies have to be found to adapt the model to the new challenges. For instance, block diagonal variance–covariance matrices could be obtained, when assuming that the spatial and temporal correlations are restricted to certain distances and time periods, respectively.

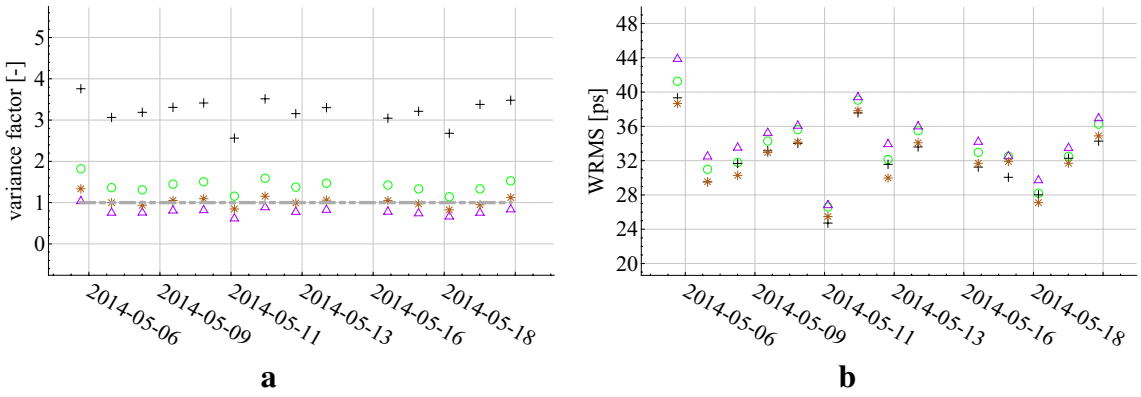

Fig. 7 χ^2 and WRMS values for a local network. **a** χ^2 values and **b** WRMS post-fit residuals for the short baseline in Hobart, Tasmania, observed during the CONT14 campaign in May 2014 and different solution setups including a reference solution (*black crosses*), a simple solution with a constant additional noise term (*purple triangles*), the Gipson et al. (2008) approach (*green circles*) and the turbulence-based solution (*brown stars*). The *gray dashed line* in **a** represents $\chi^2 = 1$

The turbulence-based model is generally suitable for different network geometries and can be used for traditional long baselines as well as for local approaches as the baseline lengths repeatabilities could be improved and the mean χ^2 values are approximately between 1 and 1.2 in all cases. However, we could see that the results in the local case are even better than those of global applications. Keeping in mind that only the turbulence model considers correlations between the co-located stations in a proper way, it becomes obvious that the differences between the results of the solution setups are larger in local VLBI applications where high spatial and temporal correlations are found. In the case of traditional VLBI sessions, the distances between the stations are significantly larger and the spatial correlations disappear almost completely and only temporal correlations between successive observations are present. Due to the fact that we used the same turbulence parametrization at both stations of a baseline, it could be expected that this assumption is valid in local but not in global applications with baseline lengths ranging up to several hundreds of kilometers. Furthermore, please note that the additional variance–covariance matrix of high-frequency atmospheric variations in the stochastic model of VLBI observations only consists for atmospheric effects but not for other uncertainty sources such as, for instance, the clock behavior. Since the VLBI observations are always differential, this effect has, of course, also more impact on long distances than on short baselines. We can conclude that using an atmospheric turbulence model in the stochastic model of geodetic VLBI data analysis leads to an improvement of the solution with regard to the baseline length repeatabilities, the χ^2 values, the WRMS post-fit residuals as well as more realistic standard deviations of the target parameters. Further investigations are, however, necessary concerning the turbulence parameters of the different stations of a baseline to guarantee the best possible characterization of the turbulence behavior over a VLBI site. Moreover, the computational costs are kept to a limited extent for common VLBI sessions, which is a not inconsiderable factor in the data analysis.

Conclusions

One main goal of this paper is to ensure an operationally sufficient method to deal with correlations between the observations due to high-frequency refractivity variations in the neutral atmosphere as the dominant error source in the VLBI data analysis. In particular, this includes that the incorporation of a fully populated variance–covariance matrix in the stochastic model of VLBI observations is feasible without too much computational effort. This was accomplished using the Kermarrec and Schön (2014) turbulence model based on the Matérn covariance family and the widely spread Kolmogorov turbulence theory. This model, originally developed for GPS carrier phases, was adapted and modified for observations of very long baseline interferometry.

The turbulence-based solution was validated against different solution strategies, including a reference solution in which no additional noise was added to the variances of the observations, an empirical model of Gipson et al. (2008) as well as an approach in which a constant additional noise term was included. In contrast to the other refining strategies, the turbulence-based model is able to describe the meteorological and climatological conditions in a more plausible way without adding arbitrary noise terms to the variances of the observations in any form.

Investigating about 2700 VLBI sessions between 1993 and 2014, we showed that the χ^2 values as an indicator whether the global test of the least-squares adjustment is fulfilled or not reduces sharply when using additional stochastic information in any form. Considering global and local applications, the best results could be obtained by the turbulence-based solution. For local application, $\chi^2 \approx 1$ is valid for all sessions, while for global networks, however, the χ^2 is only slightly too high. This can be explained by the fact that, first, only uncertainties due to refractivity fluctuations in the atmosphere are taken into account, which are the dominant but not solely error source in the VLBI data analysis, and, second, the parametrization of the turbulence-describing parameter is quite simple. For instance, we used the same turbulence parameters for both stations of a baseline, which, of course, is only valid for small network geometries. This issue has to be further investigated in the near future, but was not part of this paper.

Moreover, we showed that the baseline length repeatabilities as a general measure of accuracy of baseline length determinations improve for the turbulence-based solution. In comparison with the reference solution and other refinement strategies, up to 50 % of the baselines are improved by at least 1 mm, whereas only a few baselines are degraded. With this approach, also far more realistic standard deviations of the derived target parameters, such as station coordinates or Earth orientation parameters, were achieved.

Due to the limited computational costs for common VLBI sessions, the method is generally suited for routine data analysis and mass processing, which was one of the key objectives of this development.

Authors' contributions

SH is the corresponding author of this study and wrote the main paper. He was responsible for the VLBI-adapted and modified turbulence model as well as refining the stochastic model of VLBI observations. TA collaborated in the design and coordination of the study and was working on the implementation of the different approaches used for comparison purposes. AI helped to draft the paper and participated in its design. AN helped to draft the

manuscript and supervised the project. All authors discussed the results and commented on the manuscript at all stages. All authors read and approved the final manuscript.

Acknowledgements
S. Halsig thanks the German Research Foundation (Deutsche Forschungsgemeinschaft, DFG) for its financial support (Project No. 318/10-1). We acknowledge the use of observations provided by the International VLBI Service for Geodesy and Astrometry (IVS).

Competing interests
The authors declare that they have no competing interests.

Received: 7 March 2016 Accepted: 2 June 2016
Published online: 21 June 2016

References

Abramowitz M, Segun IA (1964) Handbook of mathematical functions. Dover Publications, New York

Altamimi Z, Collilieux X, Métivier L (2011) ITRF2008: an improved solution of the international terrestrial reference frame. J Geodesy 85(8):457–473. doi:10.1007/s00190-011-0444-4

Angermann D, Drewes H, Krügel M, Meisel B, Gerstl M, Kelm R, Müller H, Seemüller W, Tesmer V (2004) ITRS combination center at DGFI: a terrestrial reference frame realization 2003. Deutsche Geodätische Kommission Bayer Akad Wiss München, Reihe B 313:1–141. ISSN:3-7696-8593-8, ISBN:0065-5317

Batchelor GK (1950) The application of the similarity theory of turbulence to atmospheric diffusion. Q J R Meteorol Soc 76:133–146. doi:10.1002/qj.49707632804

Böckmann S, Artz T, Nothnagel A (2010) VLBI terrestrial reference frame contributions to ITRF2008. J Geodesy 84(3):201–219. doi:10.1007/s00190-009-0357-7

Böhm J, Schuh H (2004) Vienna mapping functions in VLBI analyses. Geophys Res Lett 31:L0163. doi:10.1029/2003GL018984

Crewell S, Mech M, Reinhardt T, Selbach S, Betz HD, Brocard E, Dick G, O'Connor EJ, Fischer J, Hanisch T, Hauf T, Huenerbein A, Delobbe L, Mathes A, Peters G, Wernli H, Wiegner M, Wulfmeyer V (2008) the general observation period 2007 within the priority program on quantitative precipitation forecasting: concept and first results. Meteorol Z 17(6):849–866

Davis JL, Herring TA, Shapiro II, Rogers AEE, Elgered G (1985) Geodesy by radio interferometry—effects of atmospheric modeling errors on estimates of baseline length. Radio Sci 20(6):1593–1607. doi:10.1029/RS020i006p01593

De Boor C (1978) A practical guide to splines. Applied Mathematical Sciences, vol 27. Springer, New York

Deng Z, Bender M, Zus F, Ge M, Dick G, Ramatschi M, Wickert J, Löhnert U, Schön S (2011) Validation of tropospheric slant path delays derived from single and dual frequency GPS receivers. Radio Sci. doi:10.1029/2011RS004687

Dousa J, Bennitt GV (2013) Estimation and evaluation of hourly updated global GPS Zenith total delays over ten months. GPS Solut 17(4):453–464. doi:10.1007/s10291-012-0291-7

Elgered GK (1982) Tropospheric wet path-delay measurements. IEEE Trans Antennas Prop 30(3):502–505

Fey AL, Gordon D, Jacobs CS, Ma C, Gaume RA, Arias EF, Bianco G, Boboltz DA, Böckmann S, Bolotin S, Charlot P, Collioud A, Engelhardt G, Gipson J, Gontier AM, Heinkelmann R, Kurdubov S, Lambert S, Lytvyn S, MacMillan DS, Malkin Z, Nothnagel A, Ojha R, Skurikhina E, Sokolova J, Souchay J, Sovers OJ, Tesmer V, Titov O, Wang G, Zharov V (2015) THE SECOND REALIZATION OF THE INTERNATIONAL CELESTIAL REFERENCE FRAME BY VERY LONG BASELINE INTERFEROMETRY. The Astronomical Journal 150(2) (58), doi:10.1088/0004-6256/150/2/58

Gipson J, MacMillan D, Petrov L (2008) Improved Estimation in VLBI through Better Modeling and Analysis. In: Finkelstein A, Behrend D (eds) IVS 2008 General Meeting Proceedings, "Measuring the Future", 3–6 March 2008, St. Petersburg, Russia, pp 157–162

Gipson JM (2006) Correlation Due to Station Dependent Noise in VLBI. In: Behrend D, Baver KD (eds) IVS 2006 General Meeting Proceedings, 9–11 January 2006. Conceptión, Chile, pp 286–290

Gipson JM (2007) Incorporating correlated station dependent noise improves VLBI estimates. In: Boehm J, Pany A, Schuh H (eds) Proceedings of the 18th European VLBI for geodesy and astrometry working meeting, 12–13 April 2007, Vienna, Geowissenschaftliche Mitteilungen, Heft Nr. 79, Schriftenreihe des Studienrichtung Vermessung und Geoinformation, Technische Universität Wien, pp 129–134. ISSN 1811-8380

Halsig S, Artz T, Leek J, Nothnagel A (2014) VLBI analyses using covariance information from turbulence models. In: Behrend D, Baver KD, Armstrong K (eds) IVS 2014 general meeting proceedings, "VGOS: the new VLBI network, 2–7 March 2014, Shanghai, China. Science Press, Beijing, pp 272–276. ISBN 978-7-03-042974-2

Ishimaru A (1991) Wave propagation and scattering in random media and rough surfaces. Proc IEEE 79(10):1359–1366. doi:10.1109/5.104210

Kermarrec G, Schön S (2014) On the Mátern covariance family: a proposal for modeling temporal correlations based on turbulence theory. J Geodesy 88(11):1061–1079. doi:10.1007/s00190-014-0743-7

Koch KR (2013) Parameter estimation and hypothesis testing in linear models. Springer, Berlin

Kolmogorov A (1941) The local structure of turbulence in incompressible viscous fluid for very large Reynolds' numbers. Akad Nauk SSSR Dokl 30:301–305

MacMillan DS, Ma C (1997) Atmospheric gradients and the VLBI terrestrial and celestial reference frames. Geophys Res Lett 24(4):453–456

Matérn B (1960) Spatial variation—stochastic models and their application to some problems in forest ssurvey and other sampling investigations. Meddelanden Från Statens Skogsforskningsinstitut

Niell A, Beaudoin C, Cappallo R, Corey B, Titus M (2013) First results with the GGAO12M VGOS system. In: Zubko N, Poutanen M (eds) 21st meeting of the European VLBI group for Geodesy and Astronomy, held in Espoo, Finland, March 5–8, 2013, Reports of the Finnish Geodetic Institute, pp 29–32

Nilsson T, Haas R (2010) Impact of atmospheric turbulence on geodetic very long baseline interferometry. J Geophys Res. doi:10.1029/2009JB006579

Nothnagel A, International VLBI Service for Geodesy and Astrometry (IVS) et al (2015) The IVS data input to ITRF2014. International VLBI Service for Geodesy and Astrometry. GFZ Data Services. doi:10.5880/GFZ.1.1.2015.002

Pany A, Böhm J, MacMillan D, Schuh H, Nilsson T, Wresnik J (2011) Monte Carlo simulations of the impact of troposphere, clock and measurement errors on the repeatability of VLBI positions. J Geodesy 85(1):39–50. doi:10.1007/s00190-010-0415-1

Petit G, Luzum B (2010) IERS conventions 2010. IERS technical note 35, Verlag des Bundesamtes für Kartographie und Geodäsie, Frankfurt am Main. ISSN:1019-4568

Romero-Wolf A, Jacobs CS, Ratcliff JT (2012) Effects of tropospheric spatio-temporal correlated noise on the analysis of space geodetic data. In: Behrend D, Baver KD (eds) IVS 2012 general meeting proceedings, "Launching the next-generation IVS network, 4–9 March 2012, Madrid, Spain, pp 231–235

Schön S, Brunner F (2008) Atmospheric turbulence theory applied to GPS carrier-phase data. J Geodesy 82(1):47–57. doi:10.1007/s00190-007-0156-y

Schön S, Kutterer H (2005) Realistic uncertainty measures for GPS observations. In: Sanso F (ed) A window on the future of Geodesy, International Association of Geodesy Symposia, vol 128, Springer, Berlin, Heidelberg, pp 54–59. doi:10.1007/3-540-27432-4_10

Schuh H, Behrend D (2012) VLBI: a fascinating technique for geodesy and astrometry. J Geodyn 61:68–80. doi:10.1016/j.jog.2012.07.007

Schüler T, Kronschnabel G, Plötz C, Neidhardt A, Bertarini A, Bernhart S, la Porta L, Halsig S, Nothnagel A (2015) Initial results obtained with the first TWIN VLBI radio telescope at the Geodetic Observatory Wettzell. Sensors 15(8):18,767–18,800;. doi:10.3390/s150818

Tatarskii V (1971) The effects of the turbulent atmosphere on wave propagation. NOAA (TT-68-50464)

Taylor GI (1938) The Spectrum of Turbulence. Proceedings of the Royal Society of London A: Mathematical, Physical and Engineering Sciences 164(919):476–490. doi:10.1098/rspa.1938.0032

Tesmer V (2004) Das stochastische Modell bei der VLBI-Auswertung. Dissertation, Bayerischen Akademie der Wissenschaften, München

Tesmer V, Kutterer H (2004) An advanced stochastic model for VLBI observations and its application to VLBI data analysis. In: Vandenberg NR, Baver KD (eds) IVS 2004 general meeting proceedings, 9–11 February 2004 Ottawa, Canada, pp 296–300

Treuhaft RN, Lanyi GE (1987) The effect of the dynamic wet troposphere on radio interferometric measurements. Radio Sci 22(2):251–265. doi:10.1029/RS022i002p00251

Wheelon AD (2004) Electromagnetic scintillation, vol 1. Cambridge University Press, Cambridge Books Online, Cambridge